Journal of Physics D: Applied Physics

PAPER

Enhanced forward stimulated Brillouin scattering in silicon photonic slot waveguide Bragg grating

To cite this article: Youhua Xu *et al* 2019 *J. Phys. D: Appl. Phys.* **52** 184001

IOP Publishing Journal of Physics D: Applied Physics
J. Phys. D: Appl. Phys. **52** (2019) 184001 (6pp) https://doi.org/10.1088/1361-6463/ab06d6

Enhanced forward stimulated Brillouin scattering in silicon photonic slot waveguide Bragg grating

Youhua Xu[1], Linjie Zhou[1], Liangjun Lu[1], Jianping Chen[1] and B M A Rahman[2]

[1] Shanghai Key Lab of Navigation and Location Services, State Key Laboratory of Advanced Optical Communication Systems and Networks, Shanghai Institute for Advanced Communication and Data Science, Department of Electronic Engineering, Shanghai Jiao Tong University, Shanghai 200240, People's Republic of China
[2] Department of Electrical and Electronic Engineering, City, University of London, London EC 1V 0HB, United Kingdom

E-mail: ljzhou@sjtu.edu.cn

Received 1 November 2018, revised 10 February 2019
Accepted for publication 13 February 2019
Published 28 February 2019

Abstract

We study the forward stimulated Brillouin scattering process in a suspended silicon slot waveguide Bragg grating. Full-vectorial formalism is applied to analyze the interplay of electrostriction and radiation pressure. We show that radiation pressure is the dominant factor in the proposed waveguide. The Brillouin gain strongly depends on the structural parameters and the maximum value in the order of 10^6 W^{-1} m^{-1} is obtained in the slow light regime, which is more than two orders larger than that of the stand-alone strip and slot waveguides.

Keywords: nonlinear optics, forward stimulated Brillouin scattering, silicon photonics

(Some figures may appear in colour only in the online journal)

1. Introduction

Stimulated Brillouin scattering (SBS) is an important third-order nonlinear process that results from the interaction between two optical waves and one acoustic wave [1, 2]. SBS has been extensively studied which leads to applications including distributed temperature sensing [3, 4], slow light [5–7], reconfigurable filters [8–10], optical isolators [11, 12] and lasing [13–16].

In the past few years, there has been a surge in utilizing SBS in nanoscale photonic structures. Conventionally, SBS is viewed as an intrinsic material nonlinearity which is dictated by photo-elastic constant through the thermodynamical process of electrostriction [1]. However, this paradigm breaks down within nanoscale structures as the drastically enhanced radiation pressure at the waveguide boundaries cannot be neglected anymore [17]. This new form of boundary-induced nonlinearity significantly impacts the photon–phonon interaction. Thus, electrostriction, as well as radiation pressure, can be tailored through waveguide design to control the SBS gain in nanoscale photonic structures.

The selection of waveguide material through which photons and phonons propagate is a key to harness SBS within nanoscale structures. Typically, materials with a large refractive index and a high photo-elastic constant are ideal for generating a considerable SBS gain [18]. Chalcogenide, for example, has been used to obtain a large gain in a strip waveguide [19]. Meanwhile, a silicon waveguide is expected to have a significant gain for its relatively large refractive index (about 3.5). However, it is difficult to observe the SBS process in silicon waveguides, which is mainly ascribed to the silica substrate on which silicon waveguides are usually fabricated using advanced CMOS technology. The small acoustic impedance mismatch between silicon and silica substrate leads to phonon leakage suppressing the photon–phonon interaction [18].

To conquer this problem, it is theoretically proved that a suspended silicon waveguide which is released from the silica

substrate leaving no path for external phonon loss exhibits a strong SBS gain of 10^4 W^{-1} m^{-1} for both forward and backward SBS process [20]. The nontrivial interplay between the electrostriction force and the radiation pressure gives rise to SBS gain in waveguides of hundreds of micrometers comparable to fibers of kilometers long. The feasibility of this scheme is validated through partially [21] and fully [22] suspended silicon waveguides. A further boost of the SBS gain coefficient can be realized through novel waveguide structure design. A suspended slot waveguide is predicted to generate an SBS gain of about 10^5 W^{-1} m^{-1} due to the reinforcement of radiation pressure within the narrow gap [23]. A photonic crystal waveguide suspended in air is shown to dramatically enhance the SBS nonlinearity at the Brillouin zone boundary where the group velocity is extremely low [24, 25].

In this paper, we take a step forward to investigate the forward SBS gain in a suspended silicon slot waveguide Bragg grating. 3D finite element method (FEM) is used to simulate the optical and elastic modes with full-vectorial formalism. Simulation results show that the enhanced radiation pressure force between the narrow gap along with the decreased optical group velocity drastically increases the FSBS gain to about 10^6 W^{-1} m^{-1}.

2. Theoretical model

SBS is generated by the interaction of pump and Stokes waves through an acoustic wave. Both energy and momentum are required to be conserved during the SBS process:

$$\mathbf{q} = \mathbf{k_p} - \mathbf{k_s} \tag{1}$$

$$\Omega = \omega_p - \omega_s \tag{2}$$

where $\mathbf{q}$, $\mathbf{k_p}$ and $\mathbf{k_s}$ are the wavevectors of the acoustic, pump, and Stokes waves with a frequency of Ω, ω_p, and ω_s, respectively.

Through the conservation of particle fluxes, the SBS modal gain coefficient G can be described as [20]:

$$G(\Omega) = \frac{1}{\delta z}\frac{\omega_s}{\Omega}\frac{1}{P_p P_s}\int_{\delta V} \mathbf{f}\cdot\dot{\mathbf{u}}dV \tag{3}$$

where P_p and P_s are the powers of the pump and Stokes waves propagating along the z-axis, $\dot{\mathbf{u}}$ is the displacement velocity distribution excited by the optically induced force distribution $\mathbf{f}$. The integration is taken over δV, which is in a short segment δz of the waveguide.

For periodic waveguides, the integration is taken over a unit cell along the propagating direction. Furthermore, the power of pump and Stokes waves can be expressed as a function of the optical group velocity v_g and the unit cell length a [26, 27]:

$$P_{p,s} = \frac{1}{2a}\cdot\varepsilon_0 v_g^{p,s}\int_{\delta V}\varepsilon_r(\mathbf{r})\left|\mathbf{E}_{p,s}(\mathbf{r},\omega_{p,s})\right|^2 dV. \tag{4}$$

Considering the elastic loss where the quality factor Q of the elastic response is present [28], the SBS gain of a single elastic mode in a periodic waveguide has a Lorentzian shape and a peak value of:

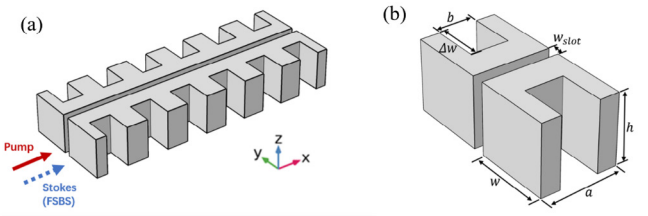

Figure 1. (a) Proposed structure of the slot waveguide Bragg grating suspended in air. (b) Unit cell of the proposed structure.

$$G(\Omega) = \frac{2a\omega Q}{\Omega^2 v_{gp} v_{gs}}\frac{\left|\langle \mathbf{f},\mathbf{u}\rangle\right|^2}{\langle \mathbf{E}_p,\varepsilon\mathbf{E}_p\rangle\langle \mathbf{E}_s,\varepsilon\mathbf{E}_s\rangle\langle \mathbf{u},\rho\mathbf{u}\rangle} \tag{5}$$

where $\langle\rangle$ denotes the integration of the inner production over a single unit cell and ρ is the mass density of the waveguide material. To simplify the calculation, the assumption is made as in [28, 29] that $\omega_p \approx \omega_s = \omega$ and $k_p \approx k_s = k$. Besides, integrals of different optical forces are linearly summed in equation (5), which allows us to investigate the SBS gain induced by different optical forces independently.

Throughout this paper, we consider two kinds of optical forces: electrostrictive body force resulting from the nonzero photo-elastic constant and radiation pressure derived from the Maxwell stress tensor (MST). The electrostriction force in a waveguide is defined as [17]:

$$F_j = -\sum_i \partial_i \sigma_{ij} \tag{6}$$

where σ_{ij} is the electrostriction stress tensor. The tensor σ_{ij} can be further expressed as:

$$\sigma_{ij} = -\frac{1}{2}\varepsilon_0 n^4 \sum_{kl} p_{ijkl} E_k E_l \tag{7}$$

where p_{ijkl} is the photo-elastic constant of the material.

The radiation pressure on the waveguide boundary between material 1 and 2 is defined as [28]:

$$F_i = (T_{2ij} - T_{1ij})\, n_j. \tag{8}$$

The MST T_{ij} in the dielectric media is expressed as:

$$T_{ij} = \varepsilon_0\varepsilon_r(x,y)\left[E_i E_j - \frac{1}{2}\delta_{ij}|E|^2\right] + \mu_0\mu_r\left[H_i H_j - \frac{1}{2}\delta_{ij}|H|^2\right] \tag{9}$$

where E and H are the electric and magnetic components of the optical field.

3. Simulation results

Using the formula depicted in section 2, we proceed to calculate the forward SBS gain coefficient in a suspended silicon slot waveguide Bragg grating. The waveguide structure is shown in figure 1(a) with a finite segment. The optical waves are tightly confined in the air slot while the elastic wave is guided within the silicon arms. In the simulation, we assume that the waveguide is axially infinite by applying Floquet boundary conditions to the unit cell shown in figure 1(b) on faces perpendicular to the propagation axis. The unit cell has

Table 1. Simulation parameters for silicon.

Refractive index n	Density ρ	Young's modulus E	Poisson's ratio ν	Photo-elastic constant $[p_{11}, p_{12}, p_{44}]$
3.5	2329 kg m^{-3}	170 × 10^9 Pa	0.28	[−0.09, 0.017, −0.051]

three symmetry planes $x = 0$, $y = 0$ and $z = 0$. We consider the case that the x-, y-, and z-axes coincide with [1 0 0], [0 1 0] and [0 0 1] symmetry directions of the monocrystalline silicon, respectively. Throughout this paper, we focus our analysis to intramode forward SBS process, where the pump and Stokes waves propagate in the same direction exciting elastic wave with wavevector $q \approx 0$ and are both in the fundamental quasi-transverse electric (quasi-TE) mode of the waveguide. Besides, the frequency range of the elastic modes is set to be below 20 GHz, which is small enough to satisfy the approximation that $\omega_p \approx \omega_s = \omega$. Simulation parameters for silicon are shown in table 1. Note that we use an isotropic Young's modulus for easy comparison with [20, 23].

To begin with, we consider a waveguide with the structure parameters as follows: $a = 315$ nm, $w = a$, $h = 0.9a$, $b = 0.5a$, $\Delta w = 0.9a$ and $w_{slot} = 0.16a$. The calculated band diagram of the fundamental quasi-TE mode is depicted in figure 2, where the shadowed area represents the light cone of air. The inset shows that the optical mode is tightly confined in the narrow gap. Due to the symmetry characteristic of the unit cell, the calculation of optical force distribution and elastic deformation only needs to be performed to one arm of the waveguide.

We select an operating point at $f = 0.203(c/a)$ $k = 0.244(2\pi/a)$ and compute the optical forces produced by the codirectionally propagating optical waves. The dominant component of the optical force is shown in figure 3, including electrostrictive body force (f^{ES}) and radiation pressure (f_y^{RP}, f_z^{RP}) on the surface. The forces are mainly in the transverse y-direction due to the dominant E_y component of the fundamental quasi-TE optical mode. This transverse nature of the optical force indicates that only elastic modes with large deformation in the y-direction are supposed to generate a considerable forward SBS gain.

Armed with the calculated force distribution, we proceed to calculate the forward SBS gain using equation (5) assuming phonon quality factor $Q = 1000$ for all elastic modes, as this Q is below the damping limit [20, 28]. Besides, we assume that the SBS process is stimulated in both arms of the waveguide, which results in a total forward SBS gain 4 times that of one arm alone [23]. As expected, only elastic modes with a large displacement in the y-direction generate effective forward SBS gain. Figure 4 shows the forward SBS gain spectrum generated by the proposed structure. The elastic mode at 12.65 GHz generates a total gain of 1743.8 W^{-1} m^{-1}, which comes from the constructive combination of radiation pressure (870.8 W^{-1} m^{-1}) and electrostriction (150 W^{-1} m^{-1}). The elastic mode at 14.53 GHz generates a total gain of 291.6 W^{-1} m^{-1} while the elastic mode at 15.95 GHz generates a total gain of 589.4 W^{-1} m^{-1}. From now on, we focus on the forward SBS gain generated by the elastic mode at 12.65 GHz

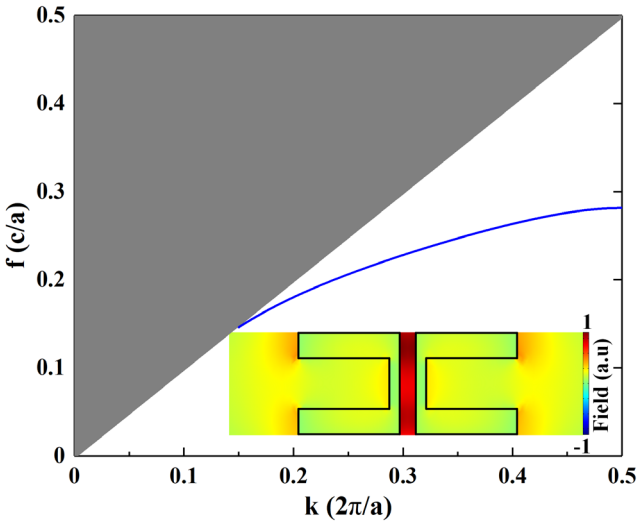

Figure 2. Band diagram of the fundamental TE-like optical mode. The inset shows the top view of the electric field E_y distribution.

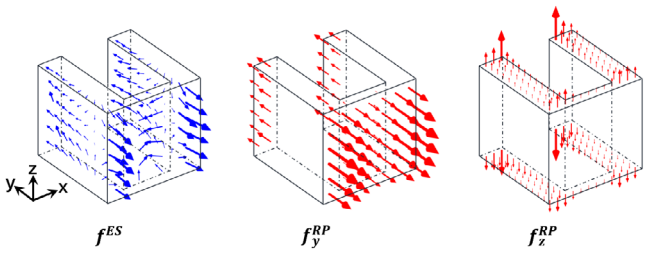

Figure 3. Distributions of electrostriction body force and radiation pressure on the surface.

due to its dominant FSBS gain and the perfect agreement between the elastic deformation shown in the inset of figure 4 and the force distribution shown in figure 3. The contribution of electrostriction is much smaller than that of radiation pressure which can be explained by the dominant optical field distribution within the air slot rather than within the silicon arms.

Next, we utilize the slow light character of the proposed suspended slot waveguide Bragg grating to further enhance the forward SBS gain. The group velocity of the TE-like optical mode can be obtained by the derivative of the dispersion relation shown in figure 2. To make use of the slow light region near the Brillouin zone boundary, we set the wavelength of the optical mode to be 1550 nm and shift the operating point along the dispersion curve. It should be noted that, with a fixed wavelength, a different operating point along the dispersion curve corresponds to a different unit cell length a [30, 31]. As shown in figure 5, as k varies from $0.2(2\pi/a)$ to $0.498(2\pi/a)$, the corresponding a varies from 279.25 nm to 436.14 nm, meanwhile, the group velocity decreases from $0.58c$ to $0.01c$. Because the structural parameters are determined by the unit cell length a, the elastic modes of different length a share the

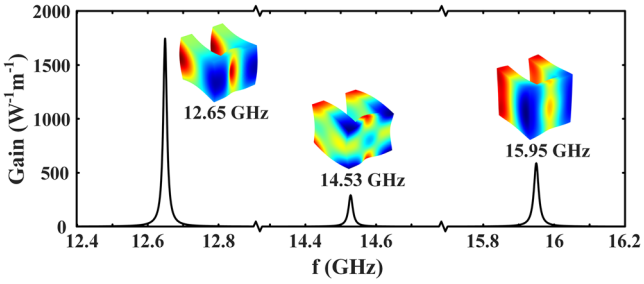

Figure 4. Forward SBS gain spectrum of the proposed structure. The coloured insets show the displacement component u_y. Red and blue correspond to positive and negative values of u_y. The deformation is proportional to the total displacement.

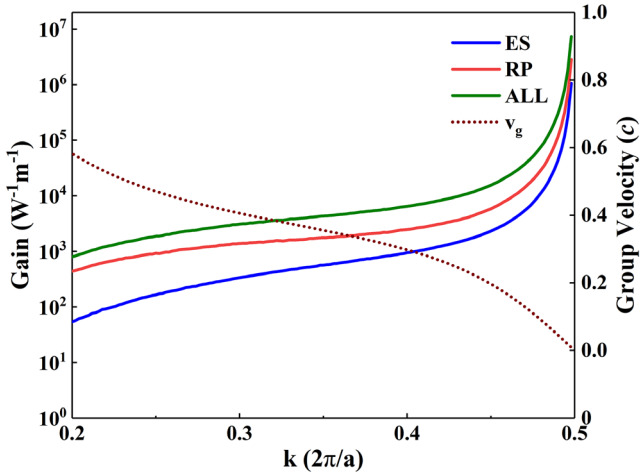

Figure 5. Forward SBS gain generated by electrostriction (blue line), radiation pressure (red line) and total gain (green line), together with the group velocity (brown dotted line) as k varies from $0.2(2\pi/a)$ to $0.5(2\pi/a)$.

identical elastic mode distribution with different frequencies. We focus our study on the specific elastic mode at 12.65 GHz when $a = 315$ nm as discussed before. The calculated forward SBS gain generated by this specific elastic mode is shown in figure 5. As can be seen, electrostriction and radiation pressure add up constructively, contributing to the total forward SBS gain. Combined with the ultra-low group velocity, these two effects lead to a total SBS gain as high as 7.33×10^6 W^{-1} m^{-1} near the Brillouin zone boundary where $k = 0.498(2\pi/a)$. Note that in order to achieve a total SBS gain larger than 10^5 W^{-1} m^{-1} at a fixed wavelength of 1550 nm, the unit cell length a has to be within 435 nm to 436.14 nm, which imposes a great challenge on device fabrication. However, the deviation of a can be compensated by shifting the working wavelength. For example, if the value a of a fabricated device deviates to 420 nm, an SBS gain of more than 10^5 W^{-1} m^{-1} can still be obtained by tuning the wavelength towards the Brillouin boundary, which is between 1492.65 nm and 1495.72 nm. This is a common method that is widely used in optical resonant devices to get the optimal operation point.

To illustrate the effect of the slow light characteristic of the proposed waveguide, we compare the forward SBS gain generated by three different structures all suspended in air: a stand-alone strip waveguide, a slot waveguide, and the

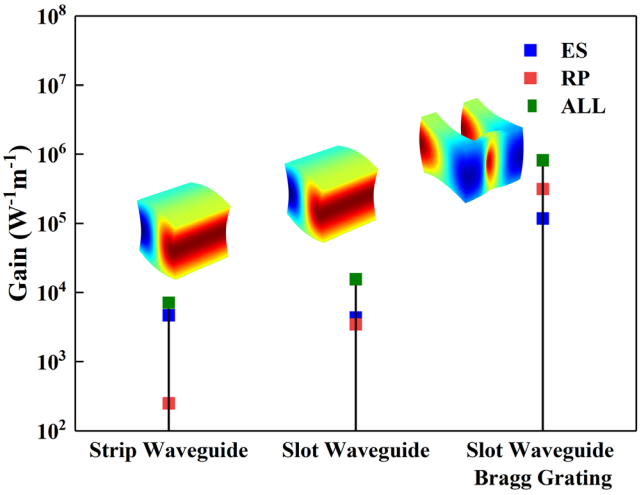

Figure 6. Forward SBS gain generated by the slow-light slot waveguide Bragg grating in comparison to a strip waveguide and a slot waveguide. The colored inset shows the displacement component u_y. Red and blue correspond to positive and negative values of u_y. The deformation is proportional to the total displacement.

proposed slot waveguide Bragg grating. The dimensions of the slot waveguide Bragg grating are $a = 436$ nm, $w = a$, $h = 0.9a$, $b = 0.5a$, $\Delta w = 0.9a$ and $w_{slot} = 0.16a$. The value of a is chosen to be 436 nm in order to satisfy the slow light condition ($k = 0.494(2\pi/a)$, $v_g = 0.028c$) of the structure at the 1550 nm wavelength. The slot waveguide Bragg grating reduces to a normal slot waveguide when the corrugation width $\Delta w = 0$. The strip waveguide is just one arm of the slot waveguide. The strip waveguide and the slot waveguide generate the largest forward SBS gain with the same elastic mode at 9.07 GHz as depicted in figure 6. Electrostriction is the dominant factor in the strip waveguide due to the large optical intensity within the silicon core, which generates a total gain of 7.12×10^3 W^{-1} m^{-1} combined with the radiation pressure. Meanwhile, the total SBS gain generated by both arms of the slot waveguide is 1.55×10^4 W^{-1} m^{-1}. However, with the same slot width, the slot waveguide Bragg grating generates an SBS gain of 8.18×10^5 W^{-1} m^{-1}, which is more than 100 and 50 times larger than that of the strip and slot waveguides, respectively. The enhancement is due to the small group velocity imposed by the Bragg grating.

To explore the influence of the waveguide height on the FSBS gain, we chose three height values to illustrate the device performance in the slow light regime. The other device dimensions are chosen as $w = a$, $b = 0.5a$, $\Delta w = 0.9a$ and $w_{slot} = 0.16a$. As shown in figure 7, the FSBS gain monotonically increases with k for all three cases. As an example, the FSBS gain is 2.97×10^5, 4.13×10^5 and 3.59×10^5 W^{-1} m^{-1} for $h = 0.9a$, $0.6a$, and $0.3a$ at $k = 0.49(2\pi/a)$ where $v_g = 0.0459c$, $0.0461c$ and $0.0543c$, respectively. The FSBS gain can be further increased to the order of 10^6 W^{-1} m^{-1} when the operation point moves closer to the Brillouin boundary.

With a certain h/a, a high FSBS gain is only attained at the corresponding optimal working wavelength. As shown in the inset of figure 7, we can choose $h = 220$ nm and $a = 366.7$ nm

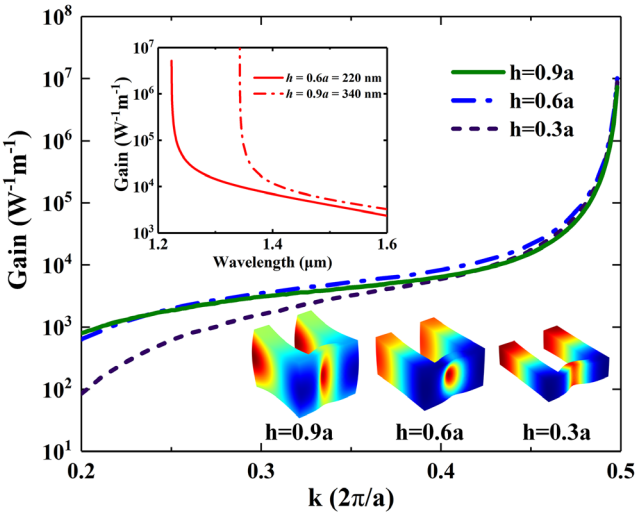

Figure 7. Forward SBS gain with three waveguide heights as k varies from $0.2(2\pi/a)$ to $0.5(2\pi/a)$. The inset shows the FSBS gain as a function of wavelength for two common SOI waveguide heights of 220 nm ($h = 0.6a$) and 340 nm ($h = 0.9a$).

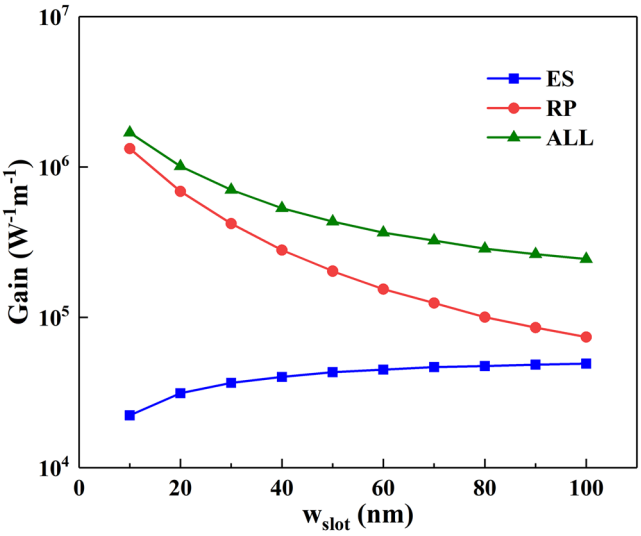

Figure 8. Forward SBS gain generated by the slow-light slot waveguide Bragg grating with a varied slot width.

($h = 0.6a$), an FSBS gain of 5.16×10^6 is achieved at the 1223.48 nm wavelength. If we choose $h = 340$ nm and $a = 377.8$ nm ($h = 0.9a$), an FSBS gain of 2.83×10^6 is reached at the 1342.73 nm wavelength. With a fixed waveguide height h, we can always adjust the unit cell length a to move the optimal working wavelength to the desired wavelength.

The slot nature of the proposed structure indicates that giant enhancement of SBS gain can be obtained by further decreasing the slot width as suggested in [23]. Here, we explore the impact of the slot width on the forward SBS gain under the same group velocity slowing down factor. The dimensions of the slot waveguide Bragg grating are $a = 436$ nm, $w = a$, $h = 0.9a$, $b = 0.5a$, $\Delta w = 0.9a$ with w_{slot} varied from 10 nm to 100 nm. We calculated the band diagram and chose the operating point at $v_g = 0.044c$ for each slot width. Figure 8 shows the scaling curves of forward SBS gain as w_{slot} varies. It can be seen that the radiation pressure becomes the dominant factor for extremely narrow slots and the total SBS gain can be further boosted by the largely enhanced radiation pressure. A total gain of 1.69×10^6 W^{-1} m^{-1} is obtained by the constructive combination of radiationis pressure (1.33×10^6 W^{-1} m^{-1}) and electrostriction (2.22×10^4 W^{-1} m^{-1}). Note that the optical frequencies at different slot widths are slightly different from each other due to the different operating point in the dispersion curve. The impact of the shifted optical frequency is negligible according to equation (5).

4. Summary

We have analyzed the forward SBS process in a periodic suspended slot waveguide Bragg grating. We show that the radiation pressure is the dominant factor with narrow slots. Electrostriction adds constructively to radiation pressure, generating a considerable forward SBS gain. Besides, the periodic structure provides a decreased group velocity near the Brillouin zone boundary. Exploiting this particular character, giant enhancement of forward SBS gain can be achieved in this waveguide. The role of the slot width is discussed, showing that further enhancement of forward SBS gain can be achieved using a narrow slot. A total gain in the order of 10^6 is attainable, which is two orders of magnitude larger than the stand-alone strip and slot waveguides. It is believed that the suspended slot waveguide in a slow-light regime provides a powerful platform for light-sound interaction through forward SBS process.

Acknowledgments

This work was partially supported by the National Natural Science Foundation of China (NSFC) (61705129, 61535006) and Shanghai Municipal Science and Technology Major Project (2017SHZDZX03).

ORCID iDs

Youhua Xu https://orcid.org/0000-0003-3621-3801

References

[1] Boyd R W and Masters B R 2009 *Nonlinear Optics* 3rd edn (New York: Academic)
[2] Chiao R Y, Townes C H and Stoicheff B P 1964 Stimulated Brillouin scattering and coherent generation of intense hypersonic waves *Phys. Rev. Lett.* **12** 592–5
[3] Kurashima T, Horiguchi T and Tateda M 1990 Distributed-temperature sensing using stimulated Brillouin scattering in optical silica fibers *Opt. Lett.* **15** 1038–40
[4] Bao X, Dhliwayo J, Heron N, Webb D J and Jackson D A 1995 Experimental and theoretical studies on a distributed temperature sensor based on Brillouin scattering *J. Lightwave Technol.* **13** 1340–8
[5] Okawachi Y, Bigelow M S, Sharping J E, Zhu Z, Schweinsberg A, Gauthier D J, Boyd R W and Gaeta A L

2005 Tunable all-optical delays via Brillouin slow light in an optical fiber *Phys. Rev. Lett.* **94** 153902
[6] Song K Y, Herráez M G and Thévenaz L 2005 Observation of pulse delaying and advancement in optical fibers using stimulated Brillouin scattering *Opt. Express* **13** 82–8
[7] Pant R, Byrnes A, Poulton C G, Li E, Choi D-Y, Madden S, Luther-Davies B and Eggleton B J 2012 Photonic-chip-based tunable slow and fast light via stimulated Brillouin scattering *Opt. Lett.* **37** 969–71
[8] Vidal B, Piqueras M A and Martí J 2007 Tunable and reconfigurable photonic microwave filter based on stimulated Brillouin scattering *Opt. Lett.* **32** 23–5
[9] Byrnes A, Pant R, Li E, Choi D-Y, Poulton C G, Fan S, Madden S, Luther-Davies B and Eggleton B J 2012 Photonic chip based tunable and reconfigurable narrowband microwave photonic filter using stimulated Brillouin scattering *Opt. Express* **20** 18836–45
[10] Kittlaus E A, Kharel P, Otterstrom N T, Wang Z and Rakich P T 2018 RF-photonic filters via on-chip photonic emit-receive operations *J. Lightwave Technol.* **36** 2803–9
[11] Huang X and Fan S 2011 Complete all-optical silica fiber isolator via stimulated Brillouin scattering *J. Lightwave Technol.* **29** 2267–75
[12] Poulton C G, Pant R, Byrnes A, Fan S, Steel M J and Eggleton B J 2012 Design for broadband on-chip isolator using stimulated Brillouin scattering in dispersion-engineered chalcogenide waveguides *Opt. Express* **20** 21235–46
[13] Stokes L F, Chodorow M and Shaw H J 1982 All-fiber stimulated Brillouin ring laser with submilliwatt pump threshold *Opt. Lett.* **7** 509–11
[14] Kabakova I V, Pant R, Choi D-Y, Debbarma S, Luther-Davies B, Madden S J and Eggleton B J 2013 Narrow linewidth Brillouin laser based on chalcogenide photonic chip *Opt. Lett.* **38** 3208–11
[15] Otterstrom N T, Behunin R O, Kittlaus E A, Wang Z and Rakich P T 2018 A silicon Brillouin laser *Science* **360** 1113–6
[16] Morrison B *et al* 2017 Compact Brillouin devices through hybrid integration on silicon *Optica* **4** 847–54
[17] Rakich P T, Davids P and Wang Z 2010 Tailoring optical forces in waveguides through radiation pressure and electrostrictive forces *Opt. Express* **18** 14439–53
[18] Eggleton B J, Poulton C G and Pant R 2013 Inducing and harnessing stimulated Brillouin scattering in photonic integrated circuits *Adv. Opt. Photonics* **5** 536–87
[19] Pant R, Poulton C G, Choi D-Y, McFarlane H, Hile S, Li E, Thevenaz L, Luther-Davies B, Madden S J and Eggleton B J 2011 On-chip stimulated Brillouin scattering *Opt. Express* **19** 8285–90
[20] Rakich P T, Reinke C, Camacho R, Davids P and Wang Z 2012 Giant enhancement of stimulated Brillouin scattering in the subwavelength limit *Phys. Rev.* X **2** 011008
[21] Van Laer R, Kuyken B, Van Thourhout D and Baets R 2015 Interaction between light and highly confined hypersound in a silicon photonic nanowire *Nat. Photon.* **9** 199
[22] Kittlaus E A, Shin H and Rakich P T 2016 Large Brillouin amplification in silicon *Nat. Photonics* **10** 463
[23] Van Laer R, Kuyken B, Van Thourhout D and Baets R 2014 Analysis of enhanced stimulated Brillouin scattering in silicon slot waveguides *Opt. Lett.* **39** 1242–5
[24] Zhang R and Sun J 2017 Design of silicon phoxonic crystal waveguides for slow light enhanced forward stimulated Brillouin scattering *J. Lightwave Technol.* **35** 2917–25
[25] Qiu W, Rakich P T, Soljacic M and Wang Z 2012 Stimulated Brillouin scattering in slow light waveguides (arXiv:1210.0738)
[26] Snyder A W and Love J D 1983 *Optical Waveguide Theory* (London: Chapman and Hall)
[27] McMillan J F, Yang X, Panoiu N C, Osgood R M and Wong C W 2006 Enhanced stimulated Raman scattering in slow-light photonic crystal waveguides *Opt. Lett.* **31** 1235–7
[28] Qiu W, Rakich P T, Shin H, Dong H, Soljačić M and Wang Z 2013 Stimulated Brillouin scattering in nanoscale silicon step-index waveguides: a general framework of selection rules and calculating SBS gain *Opt. Express* **21** 31402–19
[29] Jouybari S N 2018 Brillouin gain enhancement in nano-scale photonic waveguide *Photonics Nanostruct. Fundam. Appl.* **29** 8–14
[30] Joannopoulos J D, Johnson S G, Winn J N and Meade R D 2011 *Photonic Crystals: Molding the Flow of Light* (Princeton, NJ: Princeton University Press)
[31] Birks T, Bird D, Hedley T, Pottage J and Russell P S J 2004 Scaling laws and vector effects in bandgap-guiding fibres *Opt. Express* **12** 69–74